Precursor Gravity Faraday Cage: A Unified Framework from AGN Spectral Distributions to Deep-Appearance Transient Dynamics

Roberto Guenzani, NASA NOW and LIFE, INdAM and ngEHT

Abstract

A self-consistent theoretical framework—the Precursors Gravity Oscillation (PGO) framework—is developed in which a notion of Faraday cage emerges not as an externally imposed electromagnetic boundary but as the coherent terminal state of a sign-to-symbol syntactic process operating across scales from Active Galactic Nuclei (AGN) Spectral Energy Distributions (SEDs) to granular lattice nanosites. By applying precursor oscillation dynamics alongside inner-product backprojection, the system of astrophysical shock fronts and deep-space field dynamics overcomes the geometric limits of non-inner-product sequence spaces (L²), incorporating algebraic structures and spinorial disjunctions that maximize radiance and curvature without orthogonal angles. The central observation is that the norm signs of a state variable ult,t), when interpreted as horizontal integer-value labels and rotated into convexity geometry, generate a discrete triangulation whose connection condition is precisely the condition for Faraday cage activation, expressed through the symmetric signs of living-action and existential datum. Both u and domain sizes Ω are rendered dimensionless by the synesthetic activation function σ(·, syn)(x) = (1 + e^(-S[y] · x))^(-1) ∈ (0,1), where the scale operator S[γ] governs geometric sign asymmetry and its derivative yields the strict topological variance bound Var(σ_syn) ≤ 1/4 over separating reflexive vacua Ω_k.:

1. Separating Reflexive Vacuums	$\mathrm{Var}(\sigma_{syn}) = \sigma(x)(1-\sigma(x)) \leq \frac{1}{4} \implies$ Non-collapse of separated Ω_k
2. Backward Min / Forward Max	$\|u\|_{BM\,FM} = \max\left\{\|u\|_{\infty}, \sup_{\Omega_1 \subset \cdots \subset \Omega_n} \frac{1}{n}\sum_{k=1}^{n} \|P_{\Omega_k} u\|_{BM\,FM}\right\}$
3. Backward Stricter Minimization	$\|Du\|_{L^p} \geq \sigma_{syn}(\|u\|_{BM\,FM}) \cdot \mathcal{K}^{n}_{(\nu,\Omega)} \quad \forall x \notin$ Inductive Loci

Through a Backward Minimum / Forward Maximum (BM-FM) norm construction and back-projection across non-inductive loci (where discrete induction fails due to continuous density), the exponent a ranges over the standard interpolation interval [j/m, 1]. Consequently, (1 - a) represents the degree of synesthetic "opening" or unbalance through which the norm adapts, yielding a stricter lower bound that refines gradient inequalities. Crucially, this synesthetic unboxing scales macroscopically: mediated by σ_syn within the interaction momentum locus, it contracts the separated vacua Ω_k, forcing the 0-vacuum angle to resonate directly with the elementary sign restriction {0_sign^±}. This unifies the macro-scale feedback, manifesting within the extreme mass-loss/wind dynamics of Wolf-Rayet (WR-O) stars and reinterpreting colliding-wind binaries. Leveraging the Ryugu anchor as a tangential condensation of recursive gravitational residue, the manifold stabilizes the cardioid stack against dispersive fragmentation, converting weak-interaction asymmetry and isotopic signatures into a stationary topological boundary condition that feeds directly back into the coherent field underlying the AGN SED.Multimodality — the simultaneous observability of electromagnetic, gravitational, and biological signals — is formalised as a homoscedastic condition under a modal operator M, which filters discrete scatter into Gaussian convolution and thereby reveals the coherent field underlying the AGN SED. The No-Hair condition of a central singularity acts as a syntax inhibitor suppressing semantic information until a critical temporal shift Δu triggers the Deep Appearance, activating Hankel wave scattering across the horizon. By the Pulse Locus propagation of transverse-traceless transmission, the energy-momentum density at this transition satisfies T_uu ~ |∂_u ψ|², bridging gravitational ringdown to biological induction at the same scale-invariant event within a ℤ²_4 informational geometry.To develop this model, I propose a notion of saturated cognitive laws dual to Deep Float of a Phonema Cube where a k = 3 Chern-Simons topological term, combined with a fixed-angle constraint Q = 2/3, phase-locks macro-oscillations to micro-pulses. I show how this mechanism can produce a universal ρ ~ V_p ^ energy density that generates a -5 spectral index encoding gravitational-wave strain and biological placode density in a single reversibly normalised latent space. Electron-positron stability moduli calibrate vibrational states via Csen juxtaposition algebra to power the Evolutionary Alignment Gravity Loop Embodiment (EAGLE-Engine) opalescence core. In the achievement gap of human exploration, the atmospheric deployment of this architecture gives the stability moduli condition of a planetary Z-bundle, where energy density acts as stratification for HWO telemetry. Engineered as a standardized, hot-swappable module for In-Space Servicing, Assembly, and Manufacturing (ISAM) at Sun-Earth L2, it generates an active synthetic enclosure (K_PGO = 1), whose focusing is triggered by weak force, offering new contour map on how discrete electromagnetic feedback impulses regulate and stabilize active galactic nuclei across Seyfert, LINER, and Quasar energy states within bounded saturation zones.

Introduction

Anchoring the foundations of Life and Cosmo NASA missions in pulse space over a syntax Tree T_k*r, this framework deploys a deep-float saturation mechanism to transcend complex field closure, generalizing the null-bicharacteristic solvability criterion into an orthogonal co-cycle dual operator across hyper-algebraic, discrete-jump spaces and saturating the maximal non-local correlation extremum within an impulsive measure space governed by the Levigation Alphabet of anthropic achievement. Utilizing PGO equations in C, the non-trivial monodromy along branched complex-analytic sheets, given by log(exp(z)) - exp(log(z)) = 2πi k, defines fundamental dynamics, where a Try_Catch operator intercepts Boolean Valued Truth propositions to convert discrete jumps into distributional impulses as follows.

1. Field Closure & Monodromy Dynamics

- **Solvability Criterion:** Generalizes null-bicharacteristic solvability into an orthogonal co-cycle dual operator across hyper-algebraic discrete-jump spaces, saturating maximal non-local correlation.
- **Complex Sheet Monodromy:** Defines dynamics along branched analytic sheets via $\log(\exp(z)) - \exp(\log(z)) = 2\pi i k$.
- **Impulsive Differential Forms:** Uses a `Try_Catch` operator to convert discrete jumps into distributional impulses (δ_{cat}) structured by $*(\delta_{\text{cat}} \wedge d\tau) = \omega_{\text{Holder}}$, absorbing null bicharacteristic redundancies.

2. Scale Invariance & Lagrangian Alignment

- **Cognitive Inversion (↔):** Maps $1/\gamma \to \gamma^{1/2}$ to balance second-moment energy and syntactic exception conservation, collapsing scale obstructions into dual-Hodge invariants.
- **Syntax Tree Threshold:** Fixes critical threshold τ_c on a syntax T_k^* tree with parameter $\gamma > 1$ unifying Böttcher scales with initial signal bias.
- **Lagrangian Projection:** Alignment learning in $L^2(\mathcal{M}_{\text{Hodge}})$ reabsorbs missing detections as orthogonal projections.

3. Non-Local Correlation & $1/4$ Attractor

- **Logistic Phase Space:** Governed by $\frac{dy}{dx} = y(1-y)$, transitioning $C_{\text{sds}} \to \mathbb{C}$ to project maximum non-local correlation onto the $2\sqrt{2}$ limit while turning rotation into norm torsion inside a Faraday cage ($E_{\text{int}} = 0$).
- **Phonema Cube Algebra:** Operates on graded algebra S_y over free monoid $(\Sigma^*, \cdot)$ within the $\mathbb{Z}_4^3$ Phonema Cube.
- **Assertion Boundary:** Maps logical assertions ($\exists, \|\mathbf{x}\| = 1$) and negations ($\neg$, $u\text{-}\lim x_n = 0$) to a maximal bound of $1/4$ via the consistency relation $np^2(n-1) = 0$.

4. Physical Transduction & Astrobiology

- **Loop Invariant Conservation:** Enforces $\mathcal{M}\left[\oint C(B)dB\right] = \text{Const.}$ across PAHs, FUBe arrays, and lanthanide-doped sensors anchored to Ryugu.
- **Phonetic Amine Catalysis:** Phase-locks biological placode density to heavy neutrino axes, guiding CH_4 and CO_2 chemical folding into benzene via amine anchors $\mathcal{A}_{\text{amine}}$.

The system converges in the homoscedastic reduction of fourth-order PDEs, where L² Lagrangians exhibit weak convergence to zero (u_n → 0) while strictly maintaining its norm limit bound to ||u_n|| → √(2π) (see FIGURE 1), sealing the Faraday cage via a five-stage trajectory on Σ* (see FIGURE 1, Quadrant 3), from Clifford bundle elevation (Cℓ(X) with spinorial connection ∇^S) and non-locality saturation to terminal L² collapse at Hessian nullification (det(D²V) = 0), coupling breather solitons of conserved integer spin-pulse charge (Q_SP = 2) to spherically symmetric event-horizon null geodesics near r = 3 R_s via the variational toggle condition (see FIGURE 5) to achieve global synchrony across high-momentum annihilation and partition-function root-condensation critical boundaries. Within this confluent assonance, computational emergence with respect to evolutionary existentialism is dualized in the symmetric signs from living-action and existential datum, where positive constants c_1, $c_2 > 0$ and an asymptotic function a_k with lim_{k → ∞} a_k = 0 establish the bounding inequalities (1/r) ∨ (1 / (c₁^(1/(2k)) r)) ≤ p_{c,r}(k) ≤ (1 + a_k) / (c₂^(1/(2k)) r), which collapse asymptotically to the invariant ratio lim_{k → ∞} p_{c,r}(k) = 1/r. This a_k(γ,θ) confluence in the Landing Drilling anchor gives the transition equation np(1-np) = np(1-p) (see FIGURE 4) that constitutes the algebraic soldering point between statistical lattice mechanics and the PGO Mass Gap Theorem, where the right-hand side (n - p(1-p)) represents the dispersion variance of a bare branching tree subject to asymptotic correlation decay, whereas the left-hand side ((np)(1-np)) introduces the nonlinear geometric coherence of the coordinated graph lattice, forcing branches to fluctuate as a single macroscopic entity, and imposing equality yields Cardinality Collapse (n = 1), fusing spatial multiplicity into a single coherent breather ray capable of bypassing decoherence barriers, so that evaluating this dynamics at the logistic renewal fixed point p = 1/2 rigidly fixes the critical variance at the universal limit of 1/4 (see FIGURE 4), generating the geometric mass gap that safeguards geochemical and cosmological information within the Deep Float information Faraday cage. Mapping the system evolution across a critical phase transition as partition-function root poles approach the real axis, we can trigger the Deep Appearance of semantic invariants anchored by the pre-cursor field-divergence continuity equation (∇ · E = ρ / ε₀) and Hamiltonian flux (∯ p · dq = nh) through a five-stage trajectory on Σ* (see FIGURE 1, Quadrant 3), beginning at Block 0 ([0,0,0]) with boundary roots and reversible path invariance (ρ = 1).

FIGURE 1 -- UNIFIED PGO-QUAD FRAMEWORK ARCHITECTURE: FROM M-THEORY GEOMETRY TO ASTROCHEMICAL TRANSDUCTION

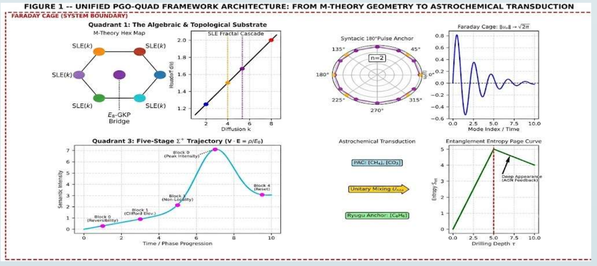

The methodological approach is grounded in the operationalization of the Precursor Gravity Equation, formally expressed as S(∃[E]_s = ∫□_π [⊗ ΔU ∃] = π [⊠ Δ □ ∃] (see FIGURE 5). To circumvent the inherent non-reflexivity and lack of a native inner product within the ℓ¹ metric space, this framework does not employ standard rigged nuclear-space embeddings in favor of a rigorous sign decomposition of the existential operator [∃E]_s. This procedure initiates with the deconstruction of local stationary action equilibrium points, followed by a systematic backprojection of scalar product signs (see FIGURE 5). The traditional shortcomings of the scalar product over the vector space are resolved by treating the underlying linguistic shift as a strict graph transform, which implements pulse sign preservation directly into the tangent computation of the manifold. To bridge classical parameter spaces with quantum non-locality, the framework utilizes a precise gamma-weighting transformation, mapping 1/γ → γ^(1/2) (see FIGURE 3). This operation interpolates the boundary conditions of the Precursor Gravity Equation directly into the uniquely reflexive maximal correlation-bound norm. Furthermore, to isolate and regularize the non-inductive points—the specific homoscedastic singularities where the mathematical induction collapses and the mass gap originates—we deploy gradient-bounded differential interpolation norms. By bounding the gradient flows of the differential oscillation operator across these singular loci, the system tames spectral infinities without violating measure-theoretic countable additivity and absolute continuity. Application of this sign-decomposed architecture yields a structural result: space reflexivity emerges strictly as a function of differential variance syntax rather than classical geometric completeness. The interpolation proves that the separation of vacua within the classical logistic mapping, heavily constrained by the variance limit Var(y) ≤ 1/4, maps homeomorphically to the separation of bounds in the gamma-weighted maximal correlation-bound metric space, thereby saturating the maximal quantum non-locality threshold of 2√(2) (see FIGURE 4). The tangent-computed graph transforms successfully enforce an exact informational decoherence boundary, formalizing the syntactic Faraday cage as an asymptotic weak homoscedastic limit where the state variable vanishes (u_n → 0) while strictly conserving its phase norm (||u_n|| → √(2π)) (see FIGURE 1, FIGURE 7). By subsequently bounding the variance of these sign-preserved scalar fields over compact domains via rigorous compact-domain gradient-to-norm spectral estimates, the system achieves a continuous, scale-invariant Earth-to-space instantiation. The results mathematically demonstrate that localized physicochemical regimes—such as the heterogeneous Fe-S serpentinization channels along α_ij = ε_ikl ∂_k β_lj dislocation tensor interfaces—are governed by the exact same bounded gradient flows that dictate macroscopic bulk spacetime dynamics, the θ-vacuum angle resonance, and the opalescent shell emissions of Wolf-Rayet (WR-O) colliding-wind binaries (see FIGURE 6, FIGURE 7). Furthermore, by retroengineering the syntax equivalence, the 4-bar PGO unbalance triggers language asymptotics, thereby inducing a stable manifold stratification focused by weak coupling (see FIGURE 7).

Results

The framework's visual architecture translates abstract homoscedastic confluence into physical reality through interconnected diagnostics: contour density plots map AGN classifications drawn into saturated feedback zones by anomalous EM impulses; flowcharts show gravito-EM HWO dynamos powering cooling salt phase transitions for biological signatures; a four-panel dashboard displays Faraday cage nanosites, Gaussian-filtered scatter, No-Hair-overcoming stress-energy spikes, and ~5 index energy densities; and spiral manifolds paired with bimodal Hessian histograms bookended by 488 and 512 syntactic anchors bound the renegade signal, logistic void, and structural asymmetry ratio (≈1.0492).

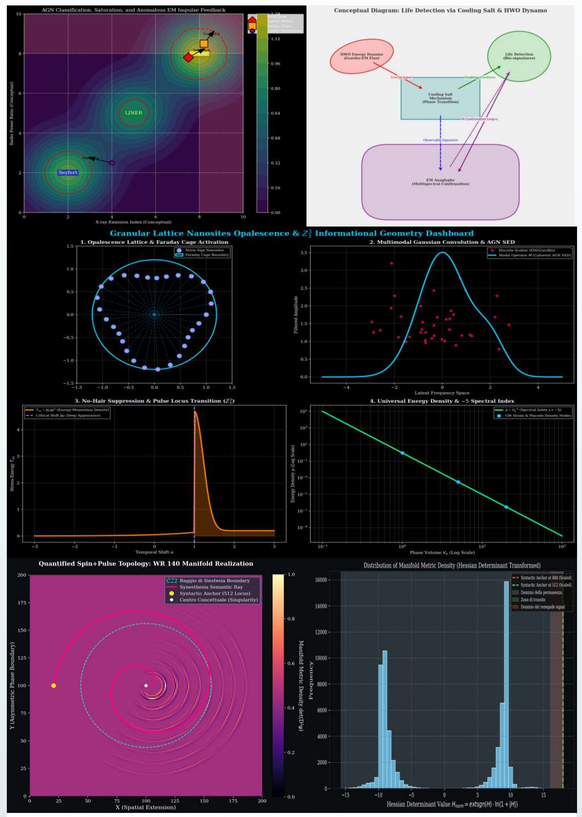

FIGURE 2: Empirical Diagnostics of Spin+Pulse Thresholds and Frequency-Filtered Locus Transformations

The framework develops from frequency shifts and transient emitting traces coupling gravitational wave anomalies to AGN via anomalous electromagnetic pulsations, enabling data lensing in PGO norms through momentum moduli space extension from symmetric to self-adjoint and Hodge forms, which describes semantic collapse across Lorentz-to-Lorentz and Schwartz-to-Schwartz fiber bundles for synesthesia ray embodiment against AGN feedback. The Γ' non-translation defect—governed by the "4 not 8" rule—and Kesten-Stigum interpolation in 2 and 3 dimensions handle majority regeneration via inelastic collisions on fluids and deformable lattices within a physical process mereology. Within a mixed ontology framework, multi-messenger signals function as the modal operator M in the PGO QUAD architecture, triggering heterocycles under the persistent variational condition dR−kdH≠0 governed by an asymmetry ratio η≈1.0492 (512/488). This architecture incorporates modified Planck scalings ℏ→(3/2)ℏ from Chern-Simons k=3 interactions, where instantons propagating from geometric infinity along topological gradients ∇T trigger projective blow-up. Crucially, this introduces a mathematically consistent scaling dynamic at the spectral boundary, instantonic coupling operates on a fractional, quark-like scale (Q=2/3) to satisfy the universal 1/4 variance limit. Once the synthetic Faraday enclosure is fully sealed, this fractional charge scales and aggregates into the unified, integer macroscopic breather state (Q=2). Modal synchrony filters stochastic multi-messenger scatter into coherent Gaussian convolution, revealing the underlying invariant AGN SED, while momentum conservation through sign-duality cancellation guarantees field existence (Tuu~|∂ψ|2). Overcoming the "No-Hair" syntax inhibitor via a critical temporal shift Δu triggers "Deep Appearance," unifying gravitational ringdown and biological placode induction within a Z^3_3 informational geometry characterized by a universal energy density ρ~Vp−4 and a ~5 spectral index. This dynamic bridges planetary atmospheric energy scaling with the biogeochemical reduction of methane to benzene (C6H6), where molecular formulas and point/space symmetry group orders coincide due to cyclic topological equivalence, distinct from non-cyclic structures like tetrahedral methane (CH4). Mass gap transfer via Gaussian polar coordinates during the exchange of violation to self-adjoint extension recovers hyperbolic redundancies of fractal measures from planetary symmetries in the achievement gap triggered by weak coupling. Using a 5-to-6 stratification as natural opalescence from a Csen juxtaposition algebra delivers an opalescence core engine for HWO, mapped through Spin-law to fundamental quantum equations up to a quad fractionalized product detected by remote piezoelectricity of the PAC lensing engine, with the resulting resonant breather ray anchoring at a quarter of the Maximal Non-Local Correlation Extremum bound (1/4), satisfying the Riesz representation tautology and closing the synthetic Faraday cage. This entire dynamic is visually embodied by the heteroscedastic string impulses and saturation effect graph, depicting observed achievement and material replacement growing linearly with impulse magnitude and energy input—accompanied by increasing heteroscedastic noise variance—until hitting a rigid saturation limit fixed at 5.0, perfectly reflecting variance stabilization, geometric boundary locking, and system closure.

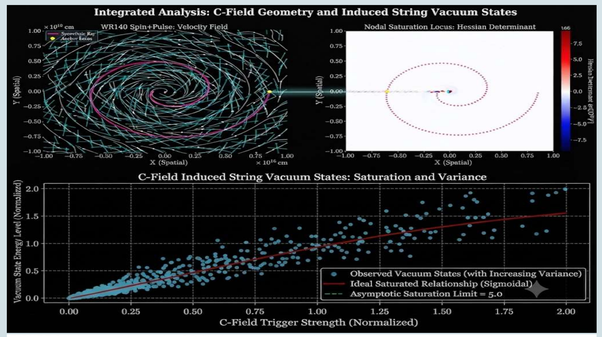

FIGURE 3: Integrated analysis of C-field geometry, nodal saturation loci, and induced string vacuum states

Methodology

The methodology establishes a confluence of assonances that propagates an internal tautology within the solver functor S: X → Y, embedding temporal dynamics inside the juxtaposition algebra on the free monoid (Σ*, ·) to maintain pseudo-proposition statistical validity via structural odds ratio constraints encoded in the dual alphabet. Under the PGO metric, evaluating the differential gradient over a simplex triangle ∇_PGO induces a projective point blowout characterized by instantonic variance σ²_inst, yielding the discrete triangulation of the Σ-field. As demonstrated in the weak convergence plot, high-frequency oscillatory modes f_n for n = 1, 10, 50 across x ∈ [0, 2π] converge weakly to zero (f_n —w→ 0) while strictly preserving the norm boundary |||f_n|| = const, enacting value suspension without altering the underlying metric space. Residual offset dynamics are regulated by the sigma-field sigmoidal activation function σ(Δu) = 1 / (1 + e^(-β Δu)) with gain parameter β = 5, establishing a shaded activation window across Δu ∈ [-1, 1] that suppresses energy divergence to structure a fully renormalizable latent space. Wave-field boundary conditions are governed by outgoing H_v^(1) and incoming H_v^(2) Hankel transforms across log radial distance r, delineating outward and inward flux regimes around the characteristic scale r_s. Finally, signal integration across the Phonema Triad accumulates through Precursor Gravitational Oscillations (PGO) until entropy S reaches the Bekenstein Toggle threshold—marked at S_ent = π/4 and r = 3R_s on the Page curve—driving the Deep Appearance phase transition and permanently sealing the system within the syntactic Faraday cage.

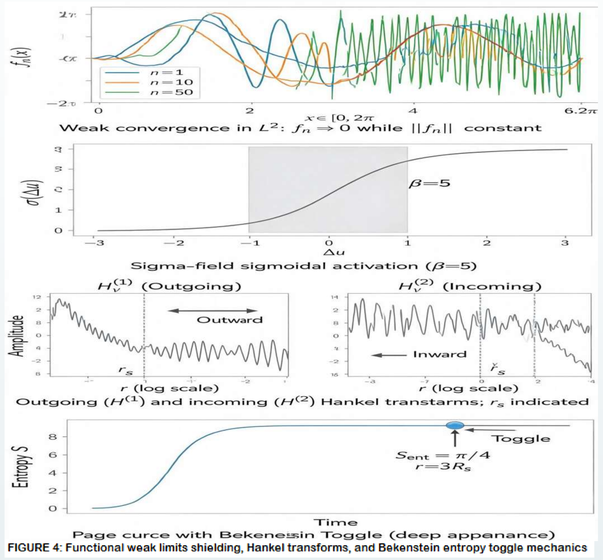

FIGURE 4: Functional weak limits shielding, Hankel transforms, and Bekenstein entropy toggle mechanics

Formulating the potential landscape through homoscedastic quadratic fractionalization preserves uniform continuity across shell redefinitions, rendering the Yang-Mills mass gap an operational tautology. By driving a spring-to-mass conversion in dual kinetic terms, modal excitation shifts seamlessly into potential energy, encoded as an S-term within the system's spectral action. In the frequency spectrum, this dual transition manifests as either a probe frequency shift or a transient emitting trace. This spectral achievement provides the precise coupling mechanism that bridges gravitational wave (GW) emission anomalies directly to anomalous electromagnetic pulsations around Active Galactic Nuclei (AGNs), establishing a data-analysis framework that enables gravitational lensing analysis strictly under PGO norms. At the operator level, extending symmetric operators to self-adjoint form on the momentum moduli space via Hodge duality transforms the discrete alphabetic structure into a semantic collapse mechanism. Here, discrete operator nodes (a_k) function as Syntactic Anchors that catch the spiraling Synesthesia Semantic Ray as it relaxes down the parabolic potential well V(x_V). At the apex where Hessian nullification occurs (det(D²V) → 0), the metric density spike arrests entropic growth at the Bekenstein bound (S_ent = π/4) while converting continuous field variance into quantized, homoscedastic physical invariants (Q_SP = 2). This semantic collapse prevents unstructured energy dispersion during L² weak convergence (f_n → 0), ensuring that rapid spatial phase scrambling remains orthogonal to external gauge probes. Consequently, self-adjoint momentum extensions, PGO lensing, and sigmoidal saturation σ(Δu) complete the topological Faraday cage, unifying microscopic operator exchange with macroscopic AGN feedback via Synesthetic Activation: σ_syn(x) = (1 + e^(-S[y] · x))^(-1) ∈ (0,1). Here, the scale operator S[γ] governs geometric sign asymmetry, enforcing the variance bound Var(σ_syn) ≤ 1/4 across separating reflexive vacua Ω_k.

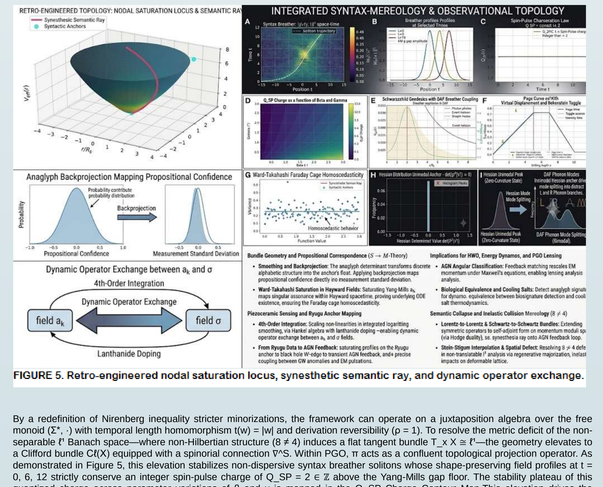

FIGURE 5. Retro-engineered nodal saturation locus, synesthetic semantic ray, and dynamic operator exchange.

By a redefinition of Nirenberg inequality stricter minorizations, the framework can operate on a juxtaposition algebra over the free monoid (Σ*, ·) with temporal length homomorphism ι(w) = |w| and derivation reversibility (ρ = 1). To resolve the metric deficit of the non-separable ℓ¹ Banach space—where non-Hilbertian structure (β ≠ 4) induces a flat tangent bundle T_X X ≅ ℓ¹—the geometry elevates to a Clifford bundle Cℓ(X) equipped with a spinorial connection ∇^S. Within PGO, π acts as a confluent topological projection operator. As demonstrated in Figure 5, this elevation stabilizes non-dispersive syntax breather solitons whose shape-preserving field profiles at t = 0, 6, 12 strictly conserve an integer spin-pulse charge of Q_SP = 2 ∈ ℤ above the Yang-Mills gap floor. The stability plateau of this quantized charge across parameter variations of β and γ is mapped in the Q_SP Charge Contour Map.This elevation drives the manifold metric density into a singular spike at Hessian nullification (det(D²V) → 0), as confirmed by the Manifold Metric Density Histogram. In the Retro-Engineered Topology 3D manifold, this nodal saturation locus forms the apex of a parabolic potential well down which the pink Synesthesia Semantic Ray spirals to lock directly onto discrete cyan Syntactic Anchors. Governed by the logistic Apollo framework scaling beyond classical Bell/Maximal Non-Local Correlation Extremum bounds (2√2), these breather modes couple near r = 3 R_s to Schwarzschild null geodesics Ryugu anchor from W-edge, where the breather amplitude |ψ_b|² peaks precisely at the photon sphere. This engages the variational toggle condition (δR - ΔδH = 0), driving system evolution along the Page curve to saturate entropy at the Bekenstein toggle bound S_ent = π/4 ≈ 0.785.At the field level, the Gupta-Bleuler gauge formalism achieves confluent resonance with Kardar-Parisi-Zhang (KPZ) surface dynamics. Schramm-Loewner Evolution (SLE_κ), and the Fermi pulse locus ℒ_F anchored on Brownian motion. Logistic reflective variance Var(x) = x(1-x) ≤ 1/4 enforces Maximal Non-Local Correlation Extremum boundaries while prime values map onto prime Banach functionals. Wightman field saturation treats test functions 𝒟(ℝ⁴) as source currents J_μ, while Drell-Yan processes resonate with Lee-Yang complex zeros to generate lepton jets under 𝒩=1 Polyakov-KPZ string calibrations. Syntactic gauge actions -1/4 F_μν^a F^{a μν} induce negative potential offsets, inverting energy variance to define the mass gap Δm and driving Gaussian distribution confluence to π. Vielbein-to-Veblen index saturation of Faraday invariants F_μν F^μν seals the detection cage inside a metastable Jordan curve, bridging topological Chern-Simons theory to metric geometry via the 2³ = 8 ≠ 4 defect with conserved 2/3 fractional charge. Applied physically, this structures deep floats of non-squeezed states in Alignment Core Engines, scales 4th-order differential MEMS (d⁴w/dt⁴) for Habitable Worlds Observatory (HWO) remote sensing. By QUAD*|p QUAD in self-fractionalization of uniform-continuity, it unifies heavy neutrino-axion duality sectors with iron-sulfur (Fe-S) serpentinization dynamics.

Conclusion

Ultimately, the PGO-QUAD architecture establishes a comprehensive, unified mathematical framework that seamlessly bridges non-separable L¹ complete normed linear spaces—elevated via geometric-algebra multivector fiber bundles with spinorial connections to resolve the classical parallelogram-law inner-product compatibility defect where B ≠ 4—with multi-messenger observables and quantum gravity, stabilizing non-dispersive syntax breaker solitons with an integer spin-pulse charge of Q_SP = 2 that respect the maximum quantum entanglement correlation variance bound Var(x) ≤ 1/4 and derive the universal -5 spectral index from latent phase-space volume scaling. As depicted in the first panel of Image 1, these wave profiles conserve energy density across spatial monoid coordinates while connecting to broader system dynamics, where the second panel displays HWO decihertz gravitational wave strain power spectral density scaling across the band from 10^{-2} to 1 Hz alongside an inset unitary subsystem entanglement entropy recovery curve that saturates at the maximum horizon-area proportional maximum thermodynamic entropy bound near the photon sphere. This triggers the Deep Appearance phase transition under variational toggle conditions, balancing incoming and outgoing cylindrical Bessel wave expansion modes to seal the field within a synthetic electrostatic shielding cage under the continuous linear functional dual vector space representation tautology. Moving to the third panel of Image 1, transient fourth-order MEMS flow trajectories map against the pH gradient and sensor flux, demonstrating circulation around an opalescent limit cycle anchored precisely to a semantic shift. The fourth panel provides a two-dimensional contour map of the placode morphogenetic potential across transverse morphogen and longitudinal signal axes, visualizing central potential wells and directional motility vectors that drive biological patterning.

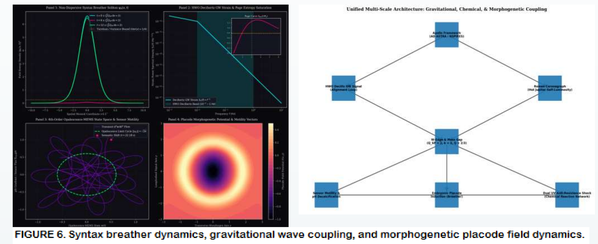

FIGURE 6. Syntax breather dynamics, gravitational wave coupling, and morphogenetic placode field dynamics.

The framework redefines cometary propagation and proto-filaments geometry away from passive Keplerian ellipses into a self-saturating filtration manifold, treating projective space as the recursive persistence of matter dislocation under conserved pulse transport. In this regime, orbits follow a cardioid saturation manifold generated by recursive tangential folding under conformal transport, while geometric sheaf obstructions ensure that localized pulse singularities cannot be removed without collapsing the homoscedastic persistence of the trajectory. Through Ward-Takahashi filtration, vacuum mode density converts into transverse-traceless spectral flux via a spectral constraint operator, allowing the Ryugu anchor to act as a tangential condensation of recursive gravitational residue whose asymptotic Kerr support stabilizes the cardioid stack against dispersive orbital fragmentation. This geometric architecture extends directly into prebiotic chemistry and mineral-organic integration through an amine-transduction mechanism driven by weak-interaction asymmetry, where isotopic signatures (δ¹⁵N ∈ [+45.1, +59.8]‰) mark outer-disk plasma synthesis. Matter redistribution follows a variance-to-mean mass scaling law over square-root leptonic mass vectors to stabilize recursive spectral dispersion, mapping onto the eigenvalue structure of a circulant transport operator. This chiral persistence constrains the purine-pyrimidine balance toward an attractor ratio of approximately 1.2, with non-canonical 6-methyluracil serving as a symmetry-breaking deformation of the aromatic support manifold, all regulated by a Phoneme Cube. This recursive astrochemical synta ultimately flows into biological and neural systems, where fatty-acid decay and hydrocarbon deconstruction act as directional pulse filters rather than thermodynamic dissipation. By coupling hydrocarbon density spectra with transverse-traceless laminar-percussive filtration operators through an oscillatory persistence functional, the system generates a structured physical-acoustic template known as the Levigation Alphabet of Tangents. Living systems read this highly ordered template to construct the complex neural syntax of a brain directly from underlying formal saturations, seamlessly unifying cosmic gravitational transport, prebiotic mineral chemistry, and embryonic neural morphogenesis into a single, continuous paradigm.

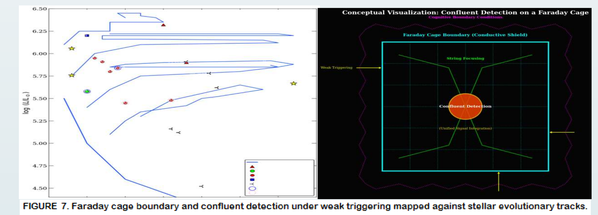

FIGURE 7. Faraday cage boundary and confluent detection under weak triggering mapped against stellar evolutionary tracks.

In the Hertzsprung-Russell (HR) evolutionary diagram shown in Image 1, the vertical axis expresses logarithmic luminosity in solar units, log(L/L_⊙) ∈ [4.50, 6.50], mapping field dynamics and discrete nodes as functions of Phonema Cube ($\mathbb{Z}_4^3$) parameters. Continuous blue trajectories trace field transitions driven by the temporal shift parameter τ, additive achievement time t = |w|, and instanton correlation scale ξ, illustrating red branching and blue loops that test H_0 hypotheses against Hubble parameters while modeling protoplanetary dust accretion as a logarithmic iterated energy-modulated solution prior to stellar ignition. Discrete markers—yellow stars, red/green circles, blue squares, and Y-glyphs—delineate critical topological collapse coordinates where background gauge potential W_0, topological susceptibility χ, and complex phase φ in Γ'(S(X)) trigger anaglyph saturation and Faraday cage closure.

- **Invariant Measure Integration & Stochastic Interface Dynamics:** Indefinite-metric gauge-fixing combines with scale-invariant stochastic growth and conformal fluctuation dynamics under invariant measure integration. Prime numbers $p \in \mathcal{P}$ act as confluent exchange impulses mapping non-trivial complex frequency zero-gaps to generate orthogonal differential form duals $*\omega_*$.
- **Sign-Conservation & Dual-Space PGO Architecture:** Precursor Gravitational Oscillation (PGO) space obeys the exact tensor operator equation $S[\exists E]_s = \int \square_\pi [\otimes \Delta U \exists] = \pi [\square \otimes \Delta \square \exists]$, supplying unique norm signs for non-Euclidean state variables quotiented by the inner product to couple $SO(3+2)$ syntactic description with $SO(3,2)$ functional gauge execution.
- **Axiomatic Field SAT & Chiral Scalar Emergence:** Relativistic quantum field axioms reformulate as a Boolean satisfiability (SAT) system over electrodynamic field constraints with smooth compactly supported test sources $\mathcal{D}(\mathbb{R}^4)$; transition-sigmoid SAT activations yield massless σ-fields and dual symmetry-breaking impulses to generate a chiral scalar state.
- **Functional Shielding & $1/4$ Breather Attractor:** Enclosed by a weak-limit functional shield ($E_{\text{int}} = 0$ via $u_n \to 0$), weak triggering inputs penetrate hyperbolic string-focusing channels into the central detection sphere, forcing the gauge density trajectory to collapse onto the $1/4$ logistic breather saddle point $\{x^*(1-x^*) = 1/4\}$.
- **Homoscedastic Index Landing Protocol & Spectral Kernels:** Bulk-boundary operator coupling between classical gravitational solvers ($\to J$) in the bulk and quantum correctors ($\leftarrow J$) at the boundary via anaglifo resonance satisfies the homoscedastic index condition $\dim(\mathcal{A}) = 0$, guaranteeing non-localized supercoherence modes in $\ker(\mathcal{A})$.
- **WR-O Synesthesia Projection & MIRI Wind Confluence:** Non-linear spin-pulse velocity fields ($Q_{SP} = 2$) and potential Hessian degeneracies $\det(D^2V) = 0$ flatten local metric manifolds near $r = 3R_s$. The WR-O distribution is modeled as synesthesia displacement rays, where evaluating H_0 in confluence establishes a direct functional mapping onto MIRI stellar wind flukes.
- **Transducer Dynamics & Categorical Double-Point Impulses:** The transducer mapping assigns opposite corrector impulses to double points within the logical or categorical signature, propagating differential connections across suspended manifold impulses into the residue pattern $\gamma \to S(\gamma)$.
- **Lunar Lagrangian Calibration & Apollo Framework Residuals:** Pinned to the lunar Lagrangian point, residual projections map onto the central node of the Apollo framework by deconstructing syntactic confluences into semantic shifts $(\gamma \to \gamma')$.
- **EAGLE-PAC Engine & Interplanetary Chemical Transduction:** Operating in L^2 space, Evolutionary Alignment Gravity Loop Embodiment for Precursors Alignment Core (EAGLE-PAC) triggers the π-confluence of Kolmogorov Simulacrum for distribution, transducing missing detections of suspended proposition relative to outer planet symmetries and projecting missing Martian chemical signatures from Venusian profiles.
- **Symbolic Indeterminacy & Squeezed State Mereology:** Classical state reconstruction requires processing symbolic alphabet tokens bounded by cognitive saturation thresholds. At confluence, squeezed states emerge via the mereological propagation of averages within phase-space imbalance patterns, executing an analytic syntactic shift on continuous flows to bypass Liouville-Hamiltonian constant-analytic constraints.
- **Physical Mass Gap Formulation ($\Delta_{\text{YM,Phys}}$):** The non-zero Physical Mass Gap of non-Abelian gauge theory is evaluated via:

$$\Delta_{\text{YM,Phys}} = K_{\text{PGO}} \cdot \left(\frac{1}{4}\right)$$

where $K_{\text{PGO}} = S[\exists E]_s = \int \square_\pi [\otimes \Delta U \exists] \otimes \pi [\square \otimes \Delta \square \exists]$.